

## **LCTV HOLOGRAPHIC IMAGING**

**Final Report  
NASA/ASEE Summer Faculty Fellowship Program - 1995  
Johnson Space Center**

**Prepared By:** Jerome Knopp, Ph.D.

**Academic Rank:** Associate Professor

**University & Department:** The University of Missouri-Columbia/Kansas City  
CEP Electrical and Computer Engineering Dept.  
Kansas City, Missouri 64110

**NASA/JSC**

**Directorate:** Engineering

**Division:** Avionic Systems

**Branch:** Electromagnetic Systems and Navigational Sensors

**JSC Colleague:** Richard D. Juday

**Date Submitted:** October 26, 1995

**Contract Number:** NGT-44-001-800

## **ABSTRACT**

Astronauts are required to interface with complex systems that require sophisticated displays to communicate effectively. Lightweight, head-mounted real-time displays that present holographic images for comfortable viewing may be the ideal solution. We describe an implementation of a liquid crystal television (LCTV) as a spatial light modulator (SLM) for the display of holograms. The implementation required the solution of a complex set of problems. These include field calculations, determination of the LCTV-SLM complex transmittance characteristics and a precise knowledge of the signal mapping between the LCTV and framegrabbing board that controls it. Realizing the hologram is further complicated by the coupling that occurs between the phase and amplitude in the LCTV transmittance. A single drive signal (a gray level signal from a framegrabber) determines both amplitude and phase. Since they are not independently controllable (as is true in the ideal SLM) one must deal with the problem of optimizing (in some sense) the hologram based on this constraint. Solutions for the above problems have been found. An algorithm has been for field calculations that uses an efficient outer product formulation. Juday's MEDOF<sup>7</sup> (Minimum Euclidean Distance Optimal Filter) algorithm used for originally for filter calculations has been successfully adapted to handle metrics appropriate for holography. This has solved the problem of optimizing the hologram to the constraints imposed by coupling. Two laboratory methods have been developed for determining an accurate mapping of framegrabber pixels to LCTV pixels. A friendly software system has been developed that integrates the hologram calculation and realization process using a simple set of instructions. The computer code and all the laboratory measurement techniques determining SLM parameters have been proven with the production of a high quality test image.

## **LCTV HOLOGRAPHIC IMAGING**

Astronauts are required to interface with complex systems that require sophisticated displays to communicate effectively. Display systems that can render 3-D objects offer significant advantages over 2-D displays for certain types of information. Holographic images with true parallax provides a high quality image that can be observed for long periods of time without the discomfort that sometimes occurs in conventional stereograms. Furthermore, a single hologram can replace a complex optical system and can reduce the weight and the number of optical components. Compact lightweight optical systems are the key to building practical head-mounted display systems that are attractive for astronaut use. Holographic displays can simultaneously incorporate the optics and the imaging device in a single element. The ideal holographic display is a high resolution spatial light modulator (SLM) with real-time imaging capability. One particular attractive and economic SLM that has real-time capability is liquid crystal television (LCTV). We describe here an implementation of an LCTV for the display of holograms. This implementation required the solution of a complex set of problems. These include field calculations, determination of the LCTV-SLM complex transmittance characteristics and a precise knowledge of the signal mapping between the LCTV and framegrabbing board that controls it. Realizing the hologram is further complicated by the coupling that occurs between the phase and amplitude of the LCTV. A single drive signal (a gray level signal from the framegrabber) determines both amplitude and phase. Since they are not independently controllable one must deal with the issue of optimizing (in some sense) the hologram based on this constraint. The solutions for these problems is discussed below.

### **MEASUREMENT OF THE LCTV COUPLING CURVE**

Before the LCTV can be used as an SLM the amplitude and phase characteristics of its complex transmittance must be determined by laboratory measurement. The LCTV screen is operated between two polarizers; the angles of the polarizers determine the SLM characteristics. Each combination of polarizer angles determines a unique SLM operating curve. The gamut of operating curves varies considerably and includes highly coupled, phase-mostly and amplitude-mostly curves. But in all cases the phase and amplitude are not independent; they are controlled by a single signal, a gray level value from a framegrabber board. In order to assure high light throughput and a bright image, the polarizers were set for phase-mostly operation. This was not necessarily the best choice of SLM curve in terms of image quality but it did assure that the image would be easy to locate. The polarizer angles for phase-mostly operation were determined by previous experiences with other LCTV cells <sup>1</sup>.

## **SLM Measurements**

The determination of the SLM curve was based on separate measurements of the amplitude and phase characteristics as a function of gray level value. The amplitude transmittance was determined from intensity transmittance measurements of a helium-neon laser beam passing through the LCTV. The relative phase transmittance was inferred from fringe shifts measurements made with a grating interferometer. This approach is described in detail elsewhere <sup>1</sup>. The shift measurements were made from framegrabbed images of fringes. In the past, ad-hoc techniques requiring a mix of computer analysis and human intervention were used to determine the shifts by examining null positions in the pattern. Because the patterns are noisy and are not uniform in amplitude variation across the fringe image the null positions can be difficult to define. This required determining null neighborhoods by eye and then using the computer to fine tune the search process. A new approach was tested that avoided the search process.

### **Algorithms for Fringe and Phase Analysis**

A first attempt was made at developing software that carried out the fringe analysis completely without human intervention. The fringe periodicity and the shift were determined using correlation. The correlations produced fairly smooth curves with clearly defined maxima and minima. The fringe pattern with the greatest contrast was used as a base on which to correlate other shifted patterns. The proper scale relation between fringe shift and phase shift was determined by an accurate measurement on the periodicity of fringe patterns. The average periodicity from the autocorrelations of all the fringe patterns gave a good estimate of the period. This was done using the Matlab m-file SMOOTH.M. The shift in the peak (global maxima) of the cross-correlation of all the patterns with the reference fringe pattern determined the relative phase shift. The technique worked well with noisy fringe data with only one caveat. The non-uniformity in the fringe contrast sometimes results in large jumps of nearly one period in the peak position due to small differences in local maxima. This was fixed by linearly interpolating phase shifts where large jumps occurred. The m-file FRINGE4.M calculated the cross-correlations and the peak shifts. The program has only been used on one data set and needs further testing. But it ran without any problems and produced data that appeared consistent with the observed fringe shift measurement estimated by ruler and eye.

## **CALCULATION OF A REALIZABLE HOLOGRAM**

Most of the past work in calculating fields for computer generated holograms is associated with farfield or Fourier transform holograms <sup>2,3</sup>. This is primarily due to the low resolution of SLMs available and the low resolution requirements

of Fourier transform holograms. There is not a significant corresponding body of work on nearfield computer generated holograms. The general problem for calculating the nearfield for an arbitrary object source is not too difficult for planar objects where the problem can be posed as a linear filter problem<sup>5</sup>. In this case the solution can be implemented on computer where the efficiencies inherent in the fast Fourier transform can be exploited. For three dimensional objects it is often more efficient to define the object as a collection of elemental objects such as points, lines, rectangular apertures, etc. and use the superposition of elemental fields to find the object field. We have chosen this approach, but have exploited approximations that lead to separability of mathematical operations in the x and y directions. This separability is inherent in field calculations for rectangular apertures and point objects modeled with quadratic approximations. This results in an efficient outer product formulations that are easy to implement in Matlab.

### The Outer Product Formulations

Calculations were made for two letter "F" objects. One defined as a collection of rectangular apertures, the other as a set of point sources. The superposed fields for the elemental objects (rectangular apertures or point sources) determines the total field for each F.

#### Rectangular Apertures

In the case of rectangular objects the fields for the rectangles were estimated using small angle (quadratic) approximations and formulated in terms of separable Fresnel integrals. The phasor field for a single rectangular aperture assumed to be transilluminated by a plane wave (or self-luminous with a uniform field across the aperture) is<sup>5</sup>:

$$U(x_o, y_o) = A \frac{e^{jkz}}{j\lambda z} \int_{-x_{lc}}^{x_{uc}} e^{\frac{jk}{2z}(x_1-x_o)^2} dx_1 \int_{-y_{lc}}^{y_{uc}} e^{\frac{jk}{2z}(y_1-y_o)^2} dy_1 \quad (1)$$

Here  $x_o, y_o$  are the coordinates of point at which the field is desired, A is a constant, z is the distance to from the observation point from the plane of the rectangular aperture, and  $\lambda$  is the wavelength and k is the propagation constant  $2\pi/\lambda$ . The limits of the integrals.  $x_{lc}, y_{lc}$ . and  $x_{uc}, y_{uc}$ . are the coordinate pairs of the lower left corner and the upper right corner of the rectangular aperture. The integrals in Eq. (1) can be redefined in terms of  $\xi, \eta$  with a change of variables defined by the following relations:

$$\frac{\pi}{2}\xi^2 = \frac{k}{2z}(x_1-x_0)^2$$

$$\frac{\pi}{2}\eta^2 = \frac{k}{2z}(y_1-y_0)^2$$

This gives:

$$U(x_0, y_0) = A \frac{e^{jkz}}{2} \int_{-\xi_1}^{\xi_2} e^{j\frac{\pi}{2}\xi^2} d\xi \int_{-\eta_1}^{\eta_2} e^{j\frac{\pi}{2}\eta^2} d\eta \quad (2)$$

The integrals in Eq. (2) are the complex form of the tabulated Fresnel integrals. Pade approximations to the Fresnel integrals are known. We used the approximation by Hastings <sup>6</sup> in the m-file FRES4.M to estimate the integrals and to calculate the fields. FRES4.M is called by the m-file FRESNEL.M which is called with the upper and lower corner coordinates of an elemental rectangular aperture as arguments. The superposition of the elemental fields (arranged to form a letter F) is given in the m-file F\_FIELD.M. The first calculations from this approach produced a field intensity that showed a diffracted and blurred projection of the letter F with fringing at the edges of the letter F. The pattern produced looked very much like the in-line holograms produced originally by Gabor <sup>4</sup>. It was decided that using this particular type of hologram might be a problem as an initial test object. Since one would observe the virtual image of the F looking through a hologram that itself resembled an F, the possibility of confusion between the image in the hologram and the virtual image exists. It was decided to use a diffusive representation of the letter F instead. The diffusive virtual image consisted of a set of randomly phased point sources arranged to form an F. The use of random phasing guaranteed a specular field intensity in the hologram plane in which the underlying structure of the F was completely hidden from the eye.

### Point Sources

Holograms resulting from point sources can be efficiently calculated using a quadratic approximation to each point source. The quadratic approximation leads to the same x-y separability that was exploited in the rectangular aperture calculations. Given a point source of strength A located at  $(x_1, y_1)$  the phasor field can be represented  $U_p$  is given by <sup>5</sup>:

$$U_p(x_o, y_o) = \frac{Ae^{jk[(x_o-x_1)^2+(y_o-y_1)^2(z_o-z_1)^2]}}{\sqrt{(x_o-x_1)^2+(y_o-y_1)^2(z_o-z_1)^2}}$$

If we assume that the point source is located near the z-axis and that the point observation makes small angles with respect to the z-axis then the field may be approximated as <sup>5</sup>:

$$U(x_o, y_o) = \frac{A}{z} e^{j\frac{k}{2z}(x_o-x_1)^2} e^{j\frac{k}{2z}(y_o-y_1)^2}$$

As in the previous case, the separability of the quadratic approximation implies that an outer product formulation is possible. The Matlab code for these calculations is in the m-file POINTHOL.M.

### Optimization of the Hologram: HOLOMED

Once a hologram has been calculated, its field must be optimally fitted to the SLM characteristics of the LCTV. The fitting process was carried out by optimizing the ratio of the light throughput of the hologram to the square error in the Euclidean distance in the complex plane between the desired complex transmittance and the realizable transmittance of the LCTV. This optimization was carried out using an adaptation of the filter program MEDOF (Minimum Euclidean Distance Optimal Filter) developed Juday <sup>7</sup>. His adaptation of MEDOF dubbed HOLOMED will be described in a future paper <sup>8</sup>. The output of the HOLOMED program is a 220(rows) X 320 array of gray level values ranging from 0 to 255. These gray level values must be written to the LCTV via a framegrabber.

### THE LCTV - FRAMEGRABBER AFFINE MAP

It would be convenient if the gray level values could be written to the LCTV with a framegrabber that mapped gray level values one to one from framegrabber pixels to LCTV pixels. This is unfortunately not case. The Matrox <sup>9</sup> PIP framegrabber used for writing to the LCTV requires a 512 X 512 array of gray level values from which a video signal is synthesized for the LCTV. Only a portion of the PIP array values are mapped to the LCTV. Rows in the PIP are converted to a standard video lines that are written to the LCTV. Odd rows and even rows separately determine the two fields that determine the interlaced image in a conventional television frame. The LCTV has only 220

rows of pixels. It overwrites the two fields on top each other; it does not interlace. Therefore 440 rows of PIP pixels are mapped to the 220 rows of the LCTV. Determining which rows in the framegrabber mapped to which lines in the LCTV was easily determined by consecutively writing "lines of pixels" (All pixels in a line set to a gray level of 255, remaining pixels to 0) from the PIP. to the LCTV and observing which PIP row first turned on the top row of pixels on the LCTV. This completely defined the row to row map. It does not define the details of the pixel mapping. Determining how pixels within a given PIP row mapped to pixels within an LCTV row was more difficult. The problem is to determine precisely where in a given line video signal from the PIP starts and stops writing to LCTV row. The start and stop points are arbitrary and there locations depend on the details of the timing circuits in the PIP and the LCTV drive electronics. This requires a measurement with subpixel accuracy. This measurement was done in two steps.

First, a rough measurement was made that resolved the start and stop positions in the framegrabber to within a framegrabber pixel. by consecutively "turning on" (i.e. set one pixel to 255, the rest to 0 ) single pixels in a framegrabber row. The effect on the LCTV screen pixels were then observed through a television microscope system. A change in the first pixel of the LCTV line. indicated the start position of PIP line writes while a change in the last LCTV pixel on the line determined the stop position for line writes. This produced a rough estimate of the. mapping ratio of PIP pixels to LCTV pixels. Two other methods were then used to fine tune the mapping between framegrabber and LCTV pixels and achieve subpixel resolution.

The first method, developed by Juday<sup>8</sup>, was based on writing a pattern of sinusoids of varying frequencies and phase shifts to the LCTV screen. The patterns were changed until a sinusoid was found that produced a uniform intensity across the LCTV of two pixels on and two pixels off. A slight error in either phase or frequency produced an easily discernable gross patten non-uniformity that was easy to see when the LCTV screen was magnified.

A second method, developed by Knopp<sup>8</sup>, was based on observing a moiré. frequency of a created by a bar pattern with a 6 pixel period. (3 pixels on, 3 pixels off) that beat with between the LCTV screen periodic pixel pattern. A low frequency beat of a few cycles across the LCTV screen was observed due to a low frequency beat in the 3rd harmonic of the periodic pattern with the LCTV pixel pitch. This permitted a fairly good measurement of the ratio of the PIP pixels to LCTV pixels. The measured ratio agreed well with the value determined by Juday's method. Although it was not done because of time constraints, it is also possible to measure phase shift by this approach by measuring the beat position. Screen uniformity can be checked by looking for any bowing in the moiré beat.



The mapping experiments yielded the following affine (line) relation between PIP pixel coordinates and LCTV coordinates:

$$t = 1.522u + 21.621$$

where  $t$  and  $u$  are PIP and LCTV pixel coordinates respectively. The equation assumes that the first pixels in a row are at 0. It can be used to remap the array coordinates of the output from HOLOMED. to pixel coordinates in the PIP. Once this inverse mapping of the desired LCTV values is determined, it is easy to determine the corresponding gray levels at pixel coordinates within the PIP. These remapped coordinates are typically "virtual" since only integer coordinate values can be realized within the framegrabber. This requires that the remapped values be interpolated using to get the actual values written to the PIP. This was done using the Matlab's cubic spline fit function. The m-file for calculating the inverse mapping and performing the interpolation is LCTVFIT.M. This subprogram is called under the m-file TVPIP.M which takes the file output from HOLOMED as an argument and produces a file that can be written directly to the PIP provided the Matlab header is stripped.

### **OBSERVATION OF THE VIRTUAL IMAGE**

The true test of all the laboratory measurements and the methodologies used to calculate fields and optimally realize them on the LCTV was the quality of the resulting image observed on the LCTV. The virtual image on the LCTV was calculated to be an F that was 6 mm high and one meter behind the LCTV. It was assumed that the hologram would be illuminated with a collimated beam from a helium-neon laser ( $\lambda = .6328$  microns). A 50 cm lens was placed about 4.5" from the LCTV and used to reimage the F on a CCD television camera. An highly astigmatic image appeared about 32 inches from the lens. The calculated distance was about 35 inches. Multiple images of the F were observed, due to the discrete grating structure of the LCTV. The error in the image location and the astigmatism were eventually led to the discovery of an error in the computer code. The pixel pitches in the x and y directions had been entered in reverse order. This error leads to severe astigmatism and errors in the image position. After correcting the coding error the astigmatism was gone. The high quality image shown in Fig. 1 was produced. Note that the point sources that make up the 'F' are clearly separated and can be used to estimate the resolution of the hologram.

### **SUMMARY AND CONCLUSIONS**

Methods of calculating and optimally realizing a hologram have been developed and proven in the laboratory. The following has been accomplished:

(1) Efficient code that uses an outer product formulation for calculating fields for objects consisting of elemental points and rectangular apertures has been developed.

(2) The MEDOF algorithm used for filter calculations has been successfully adapted to handle metrics appropriate for holography.

(3) Two laboratory methods have been developed for determining an accurate mapping of framegrabber pixels to LCTV pixels.

(4) A friendly software system has been developed that integrates the hologram calculation and realization process.

(5) The code and all the laboratory measurements on the SLM parameters has been proven with a test image.

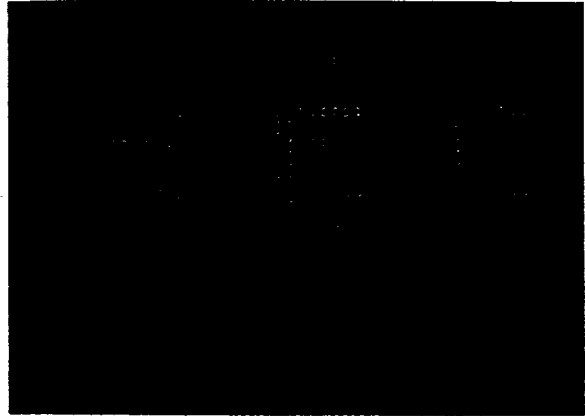


Figure 1. The image from the LCTV hologram of the letter F.

### **FUTURE RESEARCH**

A good deal of work is needed to completely exploit the hologram production system that has been developed. A possible (but far from exhaustive list) includes testing of

- (1). variations in mapping parameters
- (2). various coupling curves and their effects on images
- (3). of different hologram metrics
- (4). new SLMs
- (5). 3-D images
- (6). dynamic imagery

### **REFERENCES**

1. C. Soutar, S. E. Monroe, Jr. and J. Knopp, "Measurement of the complex transmittance of the Epson liquid crystal television", *Optical Engineering*, **33**, 1061-1068 (1994).
2. W. H. Lee, "Sampled Fourier Transform Hologram Generated by Computer", *Appl. Opt.*, **9**, 639 (1970).
3. A. W. Lohman and D.P. Paris, "Computer Generated Spatial Filters for

Coherent Data Processing", *Appl. Opt.*, **7**, 651 (1968).

4. D. Gabor, "A New Microscopic Principle", *Nature*, **161**, 777, (1948).

5. J. W. Goodman, *Introduction to Fourier Optics*, McGraw-Hill, New York (1968).

6. M. Abramowitz and I. Stegun (editors), *Handbook of Mathematical Formulas*, U.S. Department of Commerce, 7th Printing, page 300, May (1968).

7. R. D. Juday, "Optimal realizable filter minimum Euclidean distance principle", *Appl. Opt.*, **32**, 5100, (1993).

8. Details of this approach will be reported later in a paper by R.D. Juday and J. Knopp et. al. to be submitted to the *SPIE*. conference in April, Orlando, Fl. (1996) and eventually offered to *Optical Engineering*.

9. Matrox Inc., 1055 Regis Blvd., Dorval, Quebec, Canada, H9P2T4.

